Laser under ultrastrong electromagnetic interaction with matter

Motoaki Bamba* and Tetsuo Ogawa

Department of Physics, Osaka University, 1-1 Machikaneyama, Toyonaka, Osaka 560-0043, Japan
(Dated: May 19, 2015)

The conventional picture of the light amplification by stimulated emission of radiation (laser) is broken under the ultrastrong interaction between the electromagnetic fields and matter, and distinct dynamics of the electric field and of the magnetic one make the "laser" qualitatively different from the conventional laser, which has been described simply without the distinction. The "laser" in the ultrastrong regime can show a rich variety of behaviors with spontaneous appearance of coherence. We found that the "laser" generally accompanies odd-order harmonics of the electromagnetic fields both inside and outside the cavity and a synchronization with an oscillation of atomic population. A bistability is also demonstrated in a simple model under two-level and single-mode approximations.

The light and microwave amplification by stimulated emission of radiation (laser and maser) were realized in 1960 [1] and 1958 [2], respectively. Although the fundamental theory for them is established up to the quantum fluctuations of light and microwave [3–6], the discussion is performed basically under the rotating-wave approximation (RWA) on the interaction between the electromagnetic fields and matter. Under the RWA, the total number of photons and atomic excitations is conserved during the interaction, and it has enabled the simple picture based on the photons and excitations. However, the RWA fails in the ultrastrong interaction regime, that shows vacuum Rabi splitting comparable to transition frequency of the atomic excitation [7] and can now be realized in a variety of systems experimentally [8–17]. In this regime, we will see that dynamics of the electric field and of the magnetic one should be discussed distinctively due to the lack of the RWA, and we can no longer describe the laser by the stimulated emission of radiation without the distinction. Resulting from this additional degree of freedom originating from the distinction, the "laser" and "maser" in the ultrastrong regime are expected to show essential differences from the conventional laser.

The additional degree of freedom appears in the equations of the "laser" (including the meaning of "maser" in the followings), and we will see that the "laser" solutions must have multiple harmonics for satisfying them. Due to the complicated equations with the multi-harmonic expansion, we can find a rich variety of "laser" solutions that were hidden under the RWA in the conventional laser theory. In other words, the recovery of the original distinction of the electromagnetic fields in the ultrastrong regime brings out the multiple harmonics and the rich solutions. This is the conclusion of this paper, and we will show, as a demonstration, that bistable "laser" solutions are obtained even by a basic calculation.

In order to highlight the qualitative and essential aspects of the "laser" in the ultrastrong regime, we suppose an ensemble of all identical two-level atoms interacting with a single mode in a cavity of the electromagnetic fields, which has been considered to catch the basic properties of the conventional laser [3–6]. This simple system keeps the generality of the conventional laser theory, although it is known [11, 18, 19] that the finite-level and finite-mode approximations in the ultrastrong regime are not suitable for pursuing the quantitative reliability, which is obtained only by specifying a particular system of interest. Instead, the calculations in this paper are performed in two typical gauges: the Coulomb gauge and the electric-dipole one [20–23]. The qualitative and general properties should be obtained independently of the gauge choice, which however gives us quantitatively different results.

Under the two-level, single-mode, and long-wavelength approximations, the system Hamiltonians are obtained in the Coulomb and electric-dipole gauges, respectively, as [23, 24]

$$\hat{H}_{\text{Coulomb}}^{\text{cavity}} = \hbar\omega_{\text{c}}\hat{a}^{\dagger}\hat{a} + \sum_{\lambda=1}^{N} \frac{\hbar\omega_{\text{a}}}{2}\hat{\sigma}_{\lambda}^{z} + \frac{g\hbar\omega_{\text{a}}}{\sqrt{N}}(\hat{a}+\hat{a}^{\dagger})\sum_{\lambda=1}^{N}\hat{\sigma}_{\lambda}^{y}$$
$$+ g^{2}\hbar\omega_{\text{a}}\left(\hat{a}+\hat{a}^{\dagger}\right)^{2}, \tag{1}$$

$$\hat{H}_{\text{dipole}}^{\text{cavity}} = \hbar\omega_{\text{c}}\hat{a}^{\dagger}\hat{a} + \sum_{\lambda=1}^{N} \frac{\hbar\omega_{\text{a}}}{2}\hat{\sigma}_{\lambda}^{z} - \frac{ig\hbar\omega_{\text{c}}}{\sqrt{N}}(\hat{a}-\hat{a}^{\dagger})\sum_{\lambda=1}^{N}\hat{\sigma}_{\lambda}^{x}$$
$$+ \frac{g^{2}\hbar\omega_{\text{c}}}{N}\sum_{\lambda=1}^{N}\sum_{\lambda'=1}^{N}\hat{\sigma}_{\lambda}^{x}\hat{\sigma}_{\lambda'}^{x}. \tag{2}$$

Here, ω_{c} is the frequency of the cavity mode, and ω_{a} is the atomic transition frequency. $\hat{a}$ is the annihilation operator of a photon in the cavity mode and satisfies $[\hat{a},\hat{a}^{\dagger}] = 1$, while the photon does not provide a good picture in the ultrastrong regime. N is the number of atoms, and $\hat{\sigma}_{\lambda}^{x,y,z}$ is the Pauli matrix representing the λ-th atom. g is a non-dimensional interaction strength:

$$g = \sqrt{\frac{\rho|d|^{2}}{2\varepsilon_{0}\hbar\omega_{\text{c}}}}, \quad g' = g\sqrt{\frac{\omega_{\text{c}}}{\omega_{\text{a}}}} = \sqrt{\frac{\rho|d|^{2}}{2\varepsilon_{0}\hbar\omega_{\text{a}}}}, \tag{3}$$

* Present address: Department of Materials Engineering Science, Osaka University, 1-3 Machikaneyama, Toyonaka, Osaka 560-8531, Japan
E-mail: bamba@qi.mp.es.osaka-u.ac.jp

where d is the transition dipole moment of the atomic transition, ε_0 is the vacuum permittivity, and ρ is the density of atoms. In this paper, we define the ultrastrong regime as $g' \gtrsim 1$, which is determined only by the atomic parameters.

Under the RWA, the counter-rotating terms $\hat{a}\hat{\sigma}_\lambda$ and $\hat{a}^\dagger\hat{\sigma}_\lambda^\dagger$ are neglected in the interaction Hamiltonians ($\hat{\sigma}_\lambda = (\hat{\sigma}_\lambda^x - \mathrm{i}\hat{\sigma}_\lambda^y)/2$ is lowering operator of λ-th atom), and the total number of photons and atomic excitations is conserved in the remaining terms $\hat{a}^\dagger\hat{\sigma}_\lambda$ and $\hat{\sigma}_\lambda^\dagger\hat{a}$. Thanks to this simplification, in the conventional laser theory, we need to consider only the following three variables: light amplitude $\langle\hat{a}\rangle/\sqrt{N}$, atomic one $\sum_\lambda\langle\hat{\sigma}_\lambda\rangle/N$, and atomic population $Z = \sum_\lambda\langle\hat{\sigma}_\lambda^z\rangle/2N$ [3–6]. However, in the ultrastrong regime, this simple picture is no longer appropriate ($\hat{a}$ and $\hat{\sigma}_\lambda$ no longer associate positive-frequency components or lowering operators of the system) due to the lack of the RWA. Instead, we need to consider the following five variables distinctively: the non-dimensional vector potential $\mathcal{A} = \langle\hat{a} + \hat{a}^\dagger\rangle/\sqrt{N}$, electric field (or displacement) $\Pi = \mathrm{i}\langle\hat{a} - \hat{a}^\dagger\rangle/\sqrt{N}$, atomic polarization $X = \sum_\lambda\langle\hat{\sigma}_\lambda^x\rangle/2N$, current $Y = \sum_\lambda\langle\hat{\sigma}_\lambda^y\rangle/2N$, and population Z. Thanks to this distinction or the additional degrees of freedom, we can find unconventional solutions of complicated "laser" equations in the ultrastrong regime.

The inverted population is inevitable for the laser in our system even in the ultrastrong regime, and it corresponds to $Z > 0$, while $|Z| \leq 1/2$. Here, we introduce heat baths for pumping the atoms incoherently and also a bath for dissipation of the electromagnetic fields, whose couplings are mediated by $\hat{\sigma}_\lambda^x$ and $(\hat{a} + \hat{a}^\dagger)$, respectively, for suppressing the gauge-dependence [25]. Without the electromagnetic interaction with matter, each atom is incoherently pumped to Z_p with a rate $\gamma_\parallel$ [6], and the electromagnetic fields decay with a rate κ. We also consider baths for pure dephasing of atomic amplitudes X and Y (including influence of broadening of atomic transition frequencies), and they are mediated by $\hat{\sigma}_\lambda^z$ with a rate γ_pure. These dissipation rates are supposed to be frequency-independent for simplicity.

In the presence of these system-environment couplings, we derived quantum stochastic differential equations [6] based on the positive/negative frequency components [31] (see also the supplemental material [32]). For large enough $N \gg 1$ [6], macroscopic "laser" equations factorized by the above five variables are obtained in the Coulomb and electric-dipole gauges, respectively, as

$$(\partial/\partial t)\bar{\mathcal{A}} = -\omega_\mathrm{c}\bar{\Pi}, \tag{4a}$$

$$(\partial/\partial t)\bar{\Pi} = (\omega_\mathrm{c} + 4g^2\omega_\mathrm{a})\bar{\mathcal{A}} - \mathrm{i}\kappa[\bar{\mathcal{A}}^{(+)} - \bar{\mathcal{A}}^{(-)}] + 4g\omega_\mathrm{a}\bar{Y}, \tag{4b}$$

$$(\partial/\partial t)\bar{X} = -\gamma_x\bar{X} - \omega_\mathrm{a}\bar{Y} + 2g\omega_\mathrm{a}\bar{\mathcal{A}}\bar{Z}, \tag{4c}$$

$$(\partial/\partial t)\bar{Y} = \omega_\mathrm{a}\bar{X} - \gamma_y\bar{Y}, \tag{4d}$$

$$(\partial/\partial t)\bar{Z} = -\gamma_z(\bar{Z} - Z_\mathrm{p}) - 2g\omega_\mathrm{a}\bar{\mathcal{A}}\bar{X}, \tag{4e}$$

$$(\partial/\partial t)\tilde{\mathcal{A}} = -\omega_\mathrm{c}\tilde{\Pi} + 4g\omega_\mathrm{c}\tilde{X}, \tag{5a}$$

$$(\partial/\partial t)\tilde{\Pi} = \omega_\mathrm{c}\tilde{\mathcal{A}} - \mathrm{i}\kappa[\tilde{\mathcal{A}}^{(+)} - \tilde{\mathcal{A}}^{(-)}], \tag{5b}$$

$$(\partial/\partial t)\tilde{X} = -\gamma_x\tilde{X} - \omega_\mathrm{a}\tilde{Y}, \tag{5c}$$

$$(\partial/\partial t)\tilde{Y} = (\omega_\mathrm{a} - 8g^2\omega_\mathrm{c}\tilde{Z})\tilde{X} - \gamma_y\tilde{Y} + 2g\omega_\mathrm{c}\tilde{\Pi}\tilde{Z}, \tag{5d}$$

$$(\partial/\partial t)\tilde{Z} = -\gamma_z(\tilde{Z} - Z_\mathrm{p}) - 2g\omega_\mathrm{c}\tilde{\Pi}\tilde{Y} + 8g^2\omega_\mathrm{c}\tilde{X}\tilde{Y}. \tag{5e}$$

Here, the variables in the Coulomb gauge are distinguished by bar as $\bar{\mathcal{A}}$, and those in the electric-dipole gauge are distinguished by tilde as $\tilde{\mathcal{A}}$. The superscript $(\pm)$ means the positive/negative frequency component of the variables, based on which we get asymmetric dissipation rates: κ only for Π, $\gamma_x = \gamma_\mathrm{pure}$, $\gamma_y = \gamma_\parallel + \gamma_\mathrm{pure}$, and $\gamma_z = \gamma_\parallel$ [33].

In the conventional laser, the electromagnetic and atomic amplitudes ($\mathcal{A}$, Π, X, and Y) oscillate with a frequency Ω (determined for satisfying the laser equations), and the atomic population Z is constant in time. In contrast, in the ultrastrong regime, since the RWA cannot be applied to $2g\omega_\mathrm{a}\bar{\mathcal{A}}(t)\bar{X}(t)$ in Eqs. (4e) and also to $2g\omega_\mathrm{c}\tilde{\Pi}(t)\tilde{Y}(t)$ in Eq. (5e), the atomic population $\bar{Z}(t)$ and $\tilde{Z}(t)$ are driven not only by the time-constant components but also by 2Ω ones, when the amplitudes oscillate with a fundamental frequency Ω. Further, $\tilde{X}$ and $\tilde{Y}$ are driven by 3Ω components through $2g\omega_\mathrm{a}\bar{\mathcal{A}}(t)\bar{Z}(t)$ in Eq. (4c) and $2g\omega_\mathrm{c}\tilde{\Pi}(t)\tilde{Z}(t)$ in Eq. (5d), respectively. Therefore, the electromagnetic and atomic amplitudes in general oscillate with odd-order harmonics Ω, 3Ω, 5Ω, ..., and the atomic population oscillates with even-order harmonics 0Ω, 2Ω, 4Ω, ... Since the cavity loss is mediated by $\mathcal{A}$, the dynamics of the frequency components $\mathcal{A}^{(\pm)}(t)$ reflect those of the output from the cavity through the input-output relation [6, 31, 34]. Then, the output also oscillates with the odd-order harmonics. These multiple harmonics and synchronization with the atomic population are obtained in general. They are a part of the qualitative differences from the conventional laser and are obtained independently of the gauge choice.

For pursuing the simplicity, we consider only up to the third-order harmonic, which is sufficient for finding bistable "laser" solutions. The electromagnetic and atomic amplitudes are expanded as $\mathcal{A}(t) = \alpha_1 e^{-\mathrm{i}\Omega t} + \alpha_3 e^{-\mathrm{i}3\Omega t} + \mathrm{c.c.}$, $\Pi(t) = p_1 e^{-\mathrm{i}\Omega t} + p_3 e^{-\mathrm{i}3\Omega t} + \mathrm{c.c.}$ (also for X and Y), and the atomic population as $Z(t) = Z_0 + (z_2 e^{-\mathrm{i}2\Omega t} + \mathrm{c.c.})$. Neglecting highly oscillating terms (RWA in oscillation basis), non-trivial oscillating steady states are obtained from Eqs. (4) and (5) [32], and they correspond to the "laser" states.

In Fig. 1, we plot the "laser" solutions in the Coulomb gauge versus the atomic pump Z_p. The interaction strength is supposed as $g' = 0.15$, which is relevant as reported for the organic molecules [15]. We suppose the atomic dissipation rates as $\gamma_\parallel = 0.05\omega_\mathrm{a}$ and $\gamma_\mathrm{pure} = 0.1\omega_\mathrm{a}$ by considering currently available samples. The supposed cavity loss rate $\kappa = 0.01\omega_\mathrm{a}$ is lower than the one in Ref. [15], but much lower rate is available by distributed
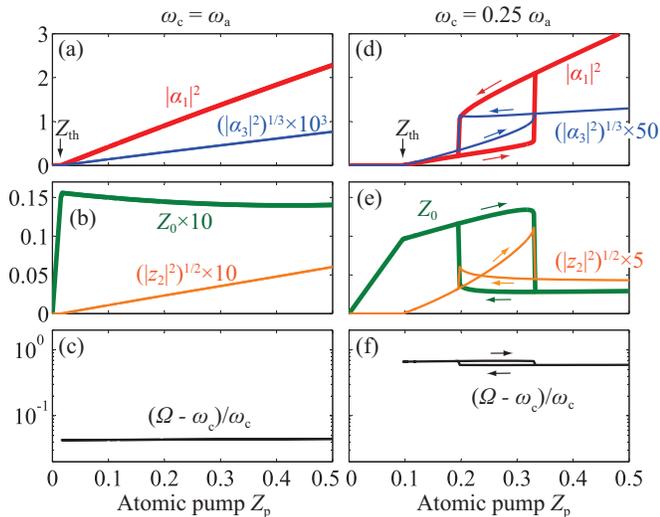
FIG. 1. "Laser" solutions are calculated with increasing and decreasing the atomic pump Z_p in the Coulomb gauge. The bare cavity frequencies are (a-c) $\omega_c = \omega_a$ and (d-f) $\omega_c = 0.25\omega_a$. (a,d) Intensities of fundamental component α_1 and 3Ω one α_3 of non-dimensional vector potential $\mathcal{A} = \langle \hat{a} + \hat{a}^\dagger \rangle / \sqrt{N}$, (b,e) time-constant component Z_0 and 2Ω one z_2 of the atomic population, and (c,f) $(\Omega - \omega_c)/\omega_c$ for fundamental oscillation frequency Ω are plotted. Below threshold $Z_p < Z_{th}$, we get $Z_0 = Z_p$ and zero oscillating components. Above threshold, we get a linear increase of $|\alpha_1|^2$, $|z_2| \propto |\alpha_1|^2$, and $|\alpha_3| = |\alpha_1|^3$ for $\omega_c = \omega_a$. A bistability appears for $\omega_c = 0.25\omega_a$. The arrows in the figures represent the solutions with increasing and decreasing Z_p. Parameters: $g' = 0.15$, $\gamma_\parallel = 0.05\omega_a$, $\gamma_{pure} = 0.1\omega_a$, and $\kappa = 0.01\omega_a$.

Bragg reflectors [35–37]. In Fig. 1(a-c), the bare cavity frequency is equal to the atomic one as $\omega_c = \omega_a$. Below the threshold $Z_{th} = 1.56 \times 10^{-2}$, the atomic population simply increases with obeying $Z = Z_0 = Z_p$, and the oscillation components are zero. Above the threshold, the intensity of the fundamental oscillation component increases linearly as $|\alpha_1|^2 \propto (Z_p - Z_{th})$ as seen in Fig. 1(a), and the time-constant component Z_0 of the atomic population is almost unchanged after the threshold as in Fig. 1(b). These are similar as the conventional laser.

The difference is the appearance of the multiple harmonics (z_2 and α_3), which are generally obtained even though higher cavity modes with $2\omega_c, 3\omega_c, \ldots$ are not considered [38]. As seen in Figs. 1(a,b), The multiple harmonics increase as $|z_2|^2 \propto (Z_p - Z_{th})^2$ and $|\alpha_3|^2 \propto (Z_p - Z_{th})^3$ as the third-order nonlinear effect (perturbation) of the fundamental component α_1.

In contrast, in Figs. 1(d-f), where the cavity frequency is far below the atomic resonance as $\omega_c = 0.25\omega_a$, we can find a bistable behavior above the threshold $Z_{th} = 9.62 \times 10^{-2}$ [39]. In Fig. 2(a), we plot the intensity $|\alpha_1|^2$ of the fundamental component calculated in the Coulomb gauge by increasing Z_p for a fixed ω_c, which is also changed in the vertical axis. When ω_c is around
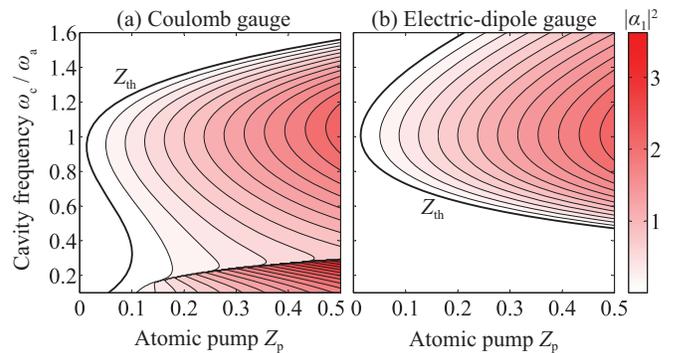

FIG. 2. Maps of "laser" solutions in (a) Coulomb gauge and (b) electric-dipole one. The intensity $|\alpha_1|^2$ of the fundamental component is calculated by increasing Z_p for a fixed ω_c, which is also changed in the vertical axis. The bold curves indicate the threshold Z_{th}. Unconventional solutions appear for low cavity frequency $\omega_c < 0.29\omega_a$ in the Coulomb gauge. Although we find only the conventional solutions in the electric-dipole gauge under the current parameters, the unconventional solutions appear for larger g' or lower κ [32]. This quantitative difference is caused by the two-level and single-mode approximations used in the calculation. Parameters: $g' = 0.15$, $\gamma_\parallel = 0.05\omega_a$, $\gamma_{pure} = 0.1\omega_a$, and $\kappa = 0.01\omega_a$.

the atomic frequency ω_a, the threshold Z_{th} is minimized and $|\alpha_1|^2$ is locally maximized. The bistability appears for low cavity frequency $0.15\omega_a < \omega_c < 0.29\omega_a$. For $\omega_c < 0.15\omega_a$, we do not find a clear jump, and the solutions change continuously (but drastically) with the increase of Z_p.

The appearance of the bistability can be understood simply by the fact that the third harmonic becomes close to the atomic resonance [$3\Omega \sim 1.2\omega_a$ in Fig. 1(d-f)]. Comparing with Fig. 1(a) ($3\Omega \sim 3.1\omega_a$), the 3Ω component α_3 is significantly enhanced in Fig. 1(d), while the fundamental one α_1 is in the same order. Thanks to the relatively large amplitudes of the multiple harmonics, we can find unconventional solutions for the complicated nonlinear equations (4) and (5) with the five variables (or more in the multi-harmonic expansion). This is the reason why the bistability appears for the low cavity frequency in Fig. 2(a). For enlarging the ω_c-range showing the "laser" down to such a low frequency, strong g', low κ, and high $\gamma_{total} = \gamma_\parallel + \gamma_{pure}$ are desired (for $\kappa < \gamma_{total}$) as expected from the conventional laser theory [3–6]. Further, low pure-dephasing ratio $\gamma_{pure}/\gamma_{total}$ ($= 2/3$ in present calculation) is advantageous to enhancing the multi-harmonic amplitudes, and then the bistability appears more clearly. This is checked numerically in supplemental material [32].

The signature of the electromagnetic distinction appears particularly in the bistable region. In the resonant case ($\omega_c = \omega_a$), the interaction is suppressed effectively through $2g\omega_a \bar{\mathcal{A}}\bar{Z}$ in Eq. (4c) and $2g\omega_c \tilde{\Pi}\tilde{Z}$ in Eq. (5d) by the negligible atomic population $Z \sim 0.01$ shown in Fig. 1(b). Then, the "laser" is reduced approxi-
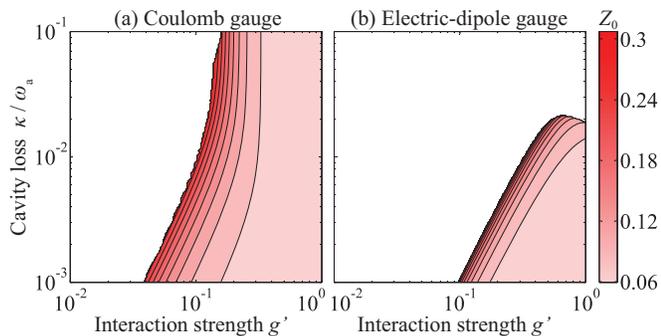
FIG. 3. The region of parameters g' and κ/ω_a showing the bistability is plotted in (a) Coulomb gauge and (b) electric-dipole one. The color indicates Z_0 (a measure of electromagnetic distinction) for the highest bare cavity frequency that shows the bistability at $Z_\text{p} = 0.5$. In both gauges, the bistability appears for strong enough interaction g' and low enough cavity loss κ. Parameters: $\gamma_\parallel = 0.05\omega_\text{a}$ and $\gamma_\text{pure} = 0.1\omega_\text{a}$.

mately to the conventional one, and the multiple harmonics appear perturbatively. In this sense, the bistability in Fig. 1(d-f) is correlated strongly to the electromagnetic distinction, because the interaction is not significantly suppressed by the atomic population $Z \sim 0.1$ as seen in Fig. 1(e). The signature of the distinction is also found in Figs. 1(c,f) showing $(\Omega - \omega_\text{c})/\omega_\text{c} = |p_1/\alpha_1| - 1$, i.e., the amplitude difference between the non-dimensional vector potential and the electric field (this relation is obtained from Eq. (4a) in the Coulomb gauge). The negligible difference $|p_1/\alpha_1| - 1 \ll 1$ in Fig. 1(c) corresponds approximately to the conventional laser, in which the photons are well defined as $|\alpha_1| = |p_1|$. In contrast, in the bistable case, the relatively large $|p_1/\alpha_1| - 1$ in Fig. 1(f) indicates that the electric field Π and the magnetic one (or vector potential $\mathcal{A}$) shows clearly distinct dynamics including the multiple harmonics. This is certainly what we initially expected in the ultrastrong regime, and the bistability originates from this distinction [40].

In Fig. 2(b), the "laser" solutions calculated in the electric-dipole gauge are plotted under the same parameters as in Fig. 2(a). Although the bistability does not appear in Fig. 2(b), it is just the quantitative difference caused by the two-level and single-mode approximations, and we can obtain the bistability even in the electric-dipole gauge for different parameters [32]. In Fig. 3, the parameter regions showing the bistability are plotted in the two gauges. We plot Z_0 in the steady state for the highest bare cavity frequency that shows the bistability for $Z_\text{p} = 0.5$ ($\omega_\text{c} = 0.29\omega_\text{a}$ in Fig. 2(a)) as functions of g' and κ. The bistability appears basically for the strong enough g' and low enough κ/ω_a, both of which is necessary for obtaining the "laser" around $3\Omega \sim \omega_\text{a}$ as discussed above. The population Z_0 is a measure of the electromagnetic distinction. The bistability starts to appear with a large Z_0, which enhances the distinction of the electromagnetic fields, and Z_0 still keeps a certain value (~ 0.06 at current parameters) even when the

bistability is easily found for large enough g'.

The quantitative difference for the appearance of the bistability mathematically originates from the following fact. As seen in Eqs. (1) and (2), the interaction terms are proportional to $g\omega_\text{a}$ and $g\omega_\text{c}$ in the Coulomb and electric-dipole gauges, respectively. Since the coefficient $g\omega_\text{a} \propto 1/\sqrt{\omega_\text{c}}$ is increased with the decrease of ω_c in the Coulomb gauge, the "laser" solution is easily found for low ω_c. As the result, the bistability is easily found in the Coulomb gauge compared to the electric-dipole one. Although this quantitative gauge-dependence is diminished if we consider all the atomic levels and the cavity modes by specifying particular systems of interest [18, 19, 42], the two-level approximation is justified qualitatively if the two atomic levels are well separated by more than $g\omega_\text{a}$ or $g\omega_\text{c}$ from the other levels energetically [43]. Since the higher cavity modes basically enhances the amplitudes of the multiple harmonics, the bistability (or multi-stability) is also expected beyond the single-mode approximations [44]. Whereas the present calculation still has such quantitative problems, the bistability is expected to appear as another qualitative difference from the conventional laser.

We conclude that, in the ultrastrong regime, the "laser" generally accompanies odd-order harmonics of the electromagnetic fields both inside and outside the cavity and the synchronization with the atomic population oscillating with even-order harmonics. Whereas we found a bistability by the calculation up to the third harmonic under the two-level and single-mode approximations, a richer variety of the "laser" solutions could be obtained thanks to the recovery of the original distinction of the electromagnetic fields in the ultrastrong regime, which exposes the additional degrees of freedom hidden by the RWA.

The properties of this "laser" are not fully elucidated in this paper, and those to be investigated spread as extensively as the conventional laser has been studied from the viewpoints of quantum optics, nonlinear physics, non-equilibrium physics, synergetics, etc. For example, it is open to dispute whether the "laser" output is in a simple coherent state as the ideal conventional laser [3–6] or a non-classical state can be directly obtained thanks to the ultrastrong interaction especially in the bistable regions [45]. Experimentally, the "laser" in the ultrastrong regime would be realized by fabricating microcavities embedding organic (dye) molecules [15] or superconducting circuits [49] with (a large number of) artificial atoms. Quantum cascade lasers involving inter-subband transitions in semiconductor quantum wells [8–11, 16] are also promising, while the present calculation does not exactly correspond to it.

ACKNOWLEDGMENTS

In App. A, we briefly explain the framework of stochastic differential equations, by which the "laser" equations in the main text are derived, and also show the Hamiltonian of system-environment couplings. The detailed calculations of the oscillating steady states from the "laser" equations are shown in Apps. B and C in the Coulomb and electric-dipole gauges, respectively. In App. D, the bistability of the "laser" in the electric-dipole gauge is demonstrated, and the dependence on the atomic decoherence is also discussed with some numerical calculations.

Appendix A: Stochastic differential equations

As a general discussion, we consider system-environment coupling expressed as

$$\hat{H}_{\text{SEC}}^{\text{example}} = \int_0^\infty d\omega \left\{ \hbar\omega \hat{f}^\dagger(\omega)\hat{f}(\omega) + i\hbar\sqrt{\frac{\Gamma(\omega)}{2\pi}}\hat{S}\left[\hat{f}^\dagger(\omega) - \hat{f}(\omega)\right] \right\}. \tag{A1}$$

Here, $\hat{S}$ is a Hermitian operator of system of interest and $\hat{f}(\omega)$ is the annihilation operator of a boson in the environment. $\Gamma(\omega)$ corresponds to the bare dissipation rate. Further, the distribution in the environment is supposed as

$$\langle \hat{f}^\dagger(\omega)\hat{f}(\omega') \rangle = n(\omega)\delta(\omega - \omega'), \tag{A2a}$$

$$\langle \hat{f}(\omega)\hat{f}^\dagger(\omega') \rangle = [n(\omega) + 1]\delta(\omega - \omega'). \tag{A2b}$$

For deriving the master equations, we usually perform the pre-trace rotating-wave approximation (RWA) to the system-environment coupling as [31]

$$\hat{H}_{\text{SEC}}^{\text{example}} \simeq \int_0^\infty d\omega \left\{ \hbar\omega \hat{f}^\dagger(\omega)\hat{f}(\omega) + i\hbar\sqrt{\frac{\Gamma(\omega)}{2\pi}}\left[\hat{f}^\dagger(\omega)\hat{s} - \hat{s}^\dagger\hat{f}(\omega)\right] \right\}, \tag{A3}$$

where $\hat{s}$ is the positive-frequency component of $\hat{S}$ defined with eigenstates $\{|\mu\rangle\}$ of system Hamiltonian $\hat{H}_0$:

$$\hat{s} = \sum_{\mu,\nu>\mu} |\mu\rangle\langle\mu|\hat{S}|\nu\rangle\langle\nu|. \tag{A4}$$

However, even from Eq. (A1) and system Hamiltonian $\hat{H}_0$, we can derive a master equation for density operator $\hat{\rho}(t)$ in the Schrödinger picture by performing partially the pre-trace RWA as [6, 31]

$$\frac{d}{dt}\hat{\rho}(t) = \frac{1}{i\hbar}\left[\hat{\rho}(t), \hat{H}_0\right] + \sum_{\mu,\nu>\mu} \frac{\Gamma(\omega_{\nu,\mu})}{2}[n(\omega_{\nu,\mu}) + 1]\left\{\left[\hat{S}, \hat{\rho}(t)\{\hat{s}_{\mu,\nu}\}^\dagger\right] + \left[\hat{s}_{\mu,\nu}\hat{\rho}(t), \hat{S}\right]\right\}$$
$$+ \sum_{\mu,\nu>\mu} \frac{\Gamma(\omega_{\nu,\mu})}{2}n(\omega_{\nu,\mu})\left\{\left[\hat{S}, \hat{\rho}(t)\hat{s}_{\mu,\nu}\right] + \left[\{\hat{s}_{\mu,\nu}\}^\dagger\hat{\rho}(t), \hat{S}\right]\right\}, \tag{A5}$$

where $\omega_{\nu,\mu}$ is the frequency difference from eigenstate $|\mu\rangle$ to $|\nu\rangle$ of $\hat{H}_0$, and $\hat{s}_{\mu,\nu}$ is defined as

$$\hat{s}_{\mu,\nu} = |\mu\rangle\langle\mu|\hat{S}|\nu\rangle\langle\nu|. \tag{A6}$$

Even in the above derivation, Eq. (A5) guarantees the thermal equilibrium $\hat{\rho} = e^{-\hat{H}_0/k_B T}$ in the steady state under the Bose distribution $n(\omega) = 1/(e^{\hbar\omega/k_B T} - 1)$ in the environment.

From Eq. (A5) for frequency-independent dissipation rate $\Gamma(\omega) = \Gamma$ and flat distribution $n(\omega) = n$, the corresponding quantum stochastic differential equation (QSDE) is obtained for system operator $\hat{O}$ in Itoh's from as [6]

$$d\hat{O} = \frac{1}{i\hbar}\left[\hat{O}, \hat{H}_0\right]dt + \frac{\Gamma(n+1)}{2}\left\{\hat{s}^\dagger[\hat{O}, \hat{S}] + [\hat{S}, \hat{O}]\hat{s}\right\}dt$$
$$+ \frac{\Gamma n}{2}\left\{\hat{s}[\hat{O}, \hat{S}] + [\hat{S}, \hat{O}]\hat{s}^\dagger\right\}dt - \sqrt{\Gamma}[\hat{O}, \hat{S}]d\hat{F}(t) + \sqrt{\Gamma}d\hat{F}^\dagger(t)[\hat{O}, \hat{S}], \tag{A7}$$

where the fluctuation operator satisfies

$$d\hat{F}(t)^2 = d\hat{F}^\dagger(t)^2 = 0 \tag{A8a}$$

$$d\hat{F}^\dagger(t)d\hat{F}(t) = n\,dt \tag{A8b}$$

$$d\hat{F}(t)d\hat{F}^\dagger(t) = (n+1)\,dt \tag{A8c}$$

When we replace $\hat{S}$ by $\hat{s}$ or $\hat{s}^\dagger$, Eq. (A7) is certainly reduced to the QSDE discussed in Ref. [6]. Since Eq. (A7) only have the commutator between $\hat{O}$ and the original Hermitian operator $\hat{S}$, we do not need the knowledge of the eigenstates of $\hat{H}_0$, which is generally hard to be calculated.

For the dissipation and incoherent pumping (by heat bath with a negative temperature [6]) of the system, we consider the following system-environment coupling

$$\hat{H}_{\text{SEC}}^x = \int_0^\infty d\omega \ \left\{ \hbar\omega \hat{f}_A^\dagger(\omega)\hat{f}_A(\omega) + i\hbar\sqrt{\frac{\kappa}{2\pi}}(\hat{a}+\hat{a}^\dagger)\left[\hat{f}_A^\dagger(\omega) - \hat{f}_A(\omega)\right] \right.$$

$$+ \hbar\sum_{\lambda=1}^N \hat{f}_{X,\lambda}^\dagger(\omega)\hat{f}_{X,\lambda}(\omega) + i\hbar\sqrt{\frac{\gamma_\parallel |Z_{\text{p}}|}{\pi}}\sum_{\lambda=1}^N \hat{\sigma}_\lambda^x\left[\hat{f}_{X,\lambda}^\dagger(\omega) - \hat{f}_{X,\lambda}(\omega)\right]$$

$$\left. + \hbar\sum_{\lambda=1}^N \hat{f}_{Z,\lambda}^\dagger(\omega)\hat{f}_{Z,\lambda}(\omega) + i\hbar\sqrt{\frac{\gamma_{\text{pure}}}{4\pi}}\sum_{\lambda=1}^N \hat{\sigma}_\lambda^z\left[\hat{f}_{Z,\lambda}^\dagger(\omega) - \hat{f}_{Z,\lambda}(\omega)\right] \right\} \tag{A9}$$

The environment fields $\hat{f}_A(\omega)$, $\hat{f}_{X,\lambda}(\omega)$, and $\hat{f}_{Z,\lambda}(\omega)$ are not correlated with each other, and their self-correlations are supposed as

$$\langle\hat{f}_A^\dagger(\omega)\hat{f}_A(\omega')\rangle = 0, \tag{A10a}$$

$$\langle\hat{f}_A(\omega)\hat{f}_A^\dagger(\omega')\rangle = \delta(\omega-\omega'), \tag{A10b}$$

$$\langle\hat{f}_{X,\lambda}^\dagger(\omega)\hat{f}_{X,\lambda'}(\omega')\rangle = \frac{1/2 + Z_{\text{p}}}{2|Z_{\text{p}}|}\delta_{\lambda,\lambda'}\delta(\omega-\omega'), \tag{A11a}$$

$$\langle\hat{f}_{X,\lambda}(\omega)\hat{f}_{X,\lambda'}^\dagger(\omega')\rangle = \frac{1/2 - Z_{\text{p}}}{2|Z_{\text{p}}|}\delta_{\lambda,\lambda'}\delta(\omega-\omega'), \tag{A11b}$$

$$\langle\hat{f}_{Z,\lambda}^\dagger(\omega)\hat{f}_{Z,\lambda'}(\omega')\rangle = 0, \tag{A12a}$$

$$\langle\hat{f}_{Z,\lambda}(\omega)\hat{f}_{Z,\lambda'}^\dagger(\omega')\rangle = \delta_{\lambda,\lambda'}\delta(\omega-\omega'). \tag{A12b}$$

From these system-environment couplings, the equations of motion of the c-number variables in the main text are derived from Eq. (A7). For the derivation, we considered that the following term is approximately zero

$$\langle\hat{\sigma}_\lambda^{x(+)}\hat{\sigma}_\lambda^z + \hat{\sigma}_\lambda^z\hat{\sigma}_\lambda^{x(+)}\rangle - \langle\hat{\sigma}_\lambda^{x(-)}\hat{\sigma}_\lambda^z + \hat{\sigma}_\lambda^z\hat{\sigma}_\lambda^{x(-)}\rangle \simeq 0. \tag{A13}$$

For deriving this, from the relations $\hat{\sigma}_\lambda^x = \hat{\sigma}_\lambda^{x(+)} + \hat{\sigma}_\lambda^{x(-)}$ and $\hat{\sigma}_\lambda^z\hat{\sigma}_\lambda^x = i\hat{\sigma}_\lambda^y$, we get the following relation

$$\langle\hat{\sigma}_\lambda^{x(+)}\hat{\sigma}_\lambda^z + \hat{\sigma}_\lambda^z\hat{\sigma}_\lambda^{x(+)}\rangle = -\langle\hat{\sigma}_\lambda^{x(-)}\hat{\sigma}_\lambda^z + \hat{\sigma}_\lambda^z\hat{\sigma}_\lambda^{x(-)}\rangle. \tag{A14}$$

The left and right hand sides oscillate mainly with positive and negative frequencies, respectively. Then, for satisfying Eq. (A14), both brackets should be zero, and Eq. (A13) can be neglected. Further, we used the following approximation

$$-\sum_{\lambda=1}^N \frac{\langle\hat{\sigma}_\lambda^{x(+)}\hat{\sigma}_\lambda^y\rangle + \langle\hat{\sigma}_\lambda^y\hat{\sigma}_\lambda^{x(+)}\rangle}{iN} \simeq 1. \tag{A15}$$

The pumping level Z_{p} is modulated by this factor in the equations of motion. When the RWA can be applied to the electromagnetic interaction with matter in the photon-excitation basis, we get $\hat{\sigma}_\lambda^{x(+)} = \hat{\sigma}_\lambda$ and $\hat{\sigma}_\lambda^{y(+)} = i\hat{\sigma}_\lambda$, then we can get the above equality. In the ultrastrong regime, the equality is generally violated. However, if we get $|Z| \ll 1$, the strength of the interaction is effectively suppressed, and $\hat{\sigma}_\lambda^{x(+)} \simeq \hat{\sigma}_\lambda$ and $\hat{\sigma}_\lambda^{y(+)} \simeq i\hat{\sigma}_\lambda$ are also obtained approximately. Even if $|Z|$ is not negligible, the atomic pump Z_{p} multiplied by Eq. (A15) shows the even-order harmonics. Further, for large enough $N \gg 1$, the deviation from the unity can be neglected in the similar way as the products of the operators are factorized under the mean-field approximation in the macroscopic laser equation.

Appendix B: Oscillating steady states in the Coulomb gauge

We decompose the five variables to frequency components as $\mathcal{A}(t) = \alpha_1 e^{-i\Omega t} + \alpha_3 e^{-i3\Omega t} + \text{c.c.}$ (Π to p_n, X to x_n, and Y to y_n), and $Z(t) = Z_0 + (z_2 e^{-i2\Omega t} + \text{c.c.})$. Then, neglecting highly oscillating terms, the equations of the frequency components are obtained in the Coulomb gauge as

$$(\partial/\partial t)\bar{\alpha}_n = in\Omega\bar{\alpha}_n - \omega_c\bar{p}_n, \tag{B1a}$$

$$(\partial/\partial t)\bar{p}_n = (\omega_c + 4g^2\omega_a - i\kappa)\bar{\alpha}_n + in\Omega\bar{p}_n + 4g\omega_a\bar{y}_n, \tag{B1b}$$

$$(\partial/\partial t)\bar{x}_1 = (i\Omega - \gamma_x)\bar{x}_1 - \omega_a\bar{y}_1 + 2g\omega_a\left(\bar{Z}_0\bar{\alpha}_1 + \bar{z}_2^*\bar{\alpha}_3 + \bar{\alpha}_1^*\bar{z}_2\right), \tag{B1c}$$

$$(\partial/\partial t)\bar{x}_3 = (i3\Omega - \gamma_x)\bar{x}_3 - \omega_a\bar{y}_3 + 2g\omega_a\left(\bar{Z}_0\bar{\alpha}_3 + \bar{\alpha}_1\bar{z}_2\right), \tag{B1d}$$

$$(\partial/\partial t)\bar{y}_n = \omega_a\bar{x}_n + (in\Omega - \gamma_y)\bar{y}_n, \tag{B1e}$$

$$(\partial/\partial t)\bar{Z}_0 = -\gamma_z\left(\bar{Z}_0 - Z_p\right) - 2g\omega_a\left(\bar{\alpha}_1^*\bar{x}_1 + \bar{\alpha}_3^*\bar{x}_3 + \text{c.c.}\right), \tag{B1f}$$

$$(\partial/\partial t)\bar{z}_2 = (i2\Omega - \gamma_z)\bar{z}_2 - 2g\omega_a\left(\bar{\alpha}_1^*\bar{x}_3 + \bar{\alpha}_1\bar{x}_1 + \bar{x}_1^*\bar{\alpha}_3\right). \tag{B1g}$$

In oscillating steady states, all of these derivatives should be zero. Equations to be satisfied are finally reduced to

$$0 = \left\{\frac{\Delta_{c,1}\Delta_{a,1}}{8g^2\omega_c\omega_a^3} + Z_p + \left[C_{|1|^21} + C_{|3|^21}|\eta|^2 + C_{(-1)^23}\eta\right]|\bar{\alpha}_1|^2\right\}\bar{\alpha}_1, \tag{B2a}$$

$$0 = \left\{\frac{\Delta_{c,3}\Delta_{a,3}}{8g^2\omega_c\omega_a^3} + Z_p + \left[C_{|1|^23} + C_{|3|^23}|\eta|^2 + C_{1^3}\eta^{-1}\right]|\bar{\alpha}_1|^2\right\}\eta\bar{\alpha}_1 e^{i2\theta}, \tag{B2b}$$

where θ is the phase of $\bar{\alpha}_1 = |\bar{\alpha}_1|e^{i\theta}$. Unknown variables are Ω, $|\bar{\alpha}_1| \in \mathbb{R}$ and a complex value

$$\eta = \frac{\bar{\alpha}_3}{\bar{\alpha}_1}e^{-i2\theta} \in \mathbb{C}. \tag{B3}$$

The other quantities in Eqs. (B2) are defined as follows

$$\Delta_{c,n} = \omega_c(\omega_c + 4g^2\omega_a) - n^2\Omega^2 - i\kappa\omega_c, \tag{B4a}$$

$$\Delta_{a,n} = \omega_a^2 + (in\Omega - \gamma_x)(in\Omega - \gamma_y), \tag{B4b}$$

$$C_{|1|^21} = -\frac{\text{Re}[(i\Omega - \gamma_y)\Delta_{c,1}]}{\gamma_z\omega_c\omega_a} + \frac{(i\Omega - \gamma_y)\Delta_{c,1}}{2\omega_c\omega_a(i2\Omega - \gamma_z)}, \tag{B5a}$$

$$C_{|3|^21} = -\frac{\text{Re}[(i3\Omega - \gamma_y)\Delta_{c,3}]}{\gamma_z\omega_c\omega_a} + \frac{(i3\Omega + \gamma_y)\Delta_{c,3}^* - (i\Omega - \gamma_y)\Delta_{c,1}}{2\omega_c\omega_a(i2\Omega + \gamma_z)}, \tag{B5b}$$

$$C_{(-1)^23} = \frac{(i3\Omega - \gamma_y)\Delta_{c,3} - (i\Omega + \gamma_y)\Delta_{c,1}^*}{2\omega_c\omega_a(i2\Omega - \gamma_z)} + \frac{(i\Omega + \gamma_y)\Delta_{c,1}^*}{2\omega_c\omega_a(i2\Omega + \gamma_z)}, \tag{B5c}$$

$$C_{|1|^23} = -\frac{\text{Re}[(i\Omega - \gamma_y)\Delta_{c,1}]}{\gamma_z\omega_c\omega_a} + \frac{(i3\Omega - \gamma_y)\Delta_{c,3} - (i\Omega + \gamma_y)\Delta_{c,1}^*}{2\omega_c\omega_a(i2\Omega - \gamma_z)}, \tag{B5d}$$

$$C_{|3|^23} = -\frac{\text{Re}[(i3\Omega - \gamma_y)\Delta_{c,3}]}{\gamma_z\omega_c\omega_a}, \tag{B5e}$$

$$C_{1^3} = \frac{(i\Omega - \gamma_y)\Delta_{c,1}}{2\omega_c\omega_a(i2\Omega - \gamma_z)}. \tag{B5f}$$

Once we get a solution of Eqs. (B2), the other frequency components are obtained as

$$\bar{\alpha}_3 = \eta\bar{\alpha}_1 e^{i2\theta}, \tag{B6a}$$

$$\bar{p}_n = \frac{in\Omega}{\omega_c}\bar{\alpha}_n, \tag{B6b}$$

$$\bar{x}_n = \frac{(in\Omega - \gamma_y)\Delta_{c,n}}{4g\omega_c\omega_a^2}\bar{\alpha}_n, \tag{B6c}$$

$$\bar{y}_n = -\frac{\omega_a}{in\Omega - \gamma_y}\bar{x}_n, \tag{B6d}$$

$$\bar{Z}_0 = Z_p - \frac{2g\omega_a}{\gamma_z}\left(\bar{\alpha}_1^*\bar{x}_1 + \bar{\alpha}_3^*\bar{x}_3 + \text{c.c.}\right), \tag{B6e}$$

$$\bar{z}_2 = \frac{2g\omega_a}{(i2\Omega - \gamma_z)}\left(\bar{\alpha}_1^*\bar{x}_3 + \bar{\alpha}_1\bar{x}_1 + \bar{x}_1^*\bar{\alpha}_3\right), \tag{B6f}$$

while the phase θ of $\bar{\alpha}_1$ can be chosen arbitrarily.

Appendix C: Oscillating steady states in the electric-dipole gauge

In the same manner as in the Coulomb gauge, the equations of the frequency components are obtained in the electric-dipole gauge as

$$(\partial/\partial t)\tilde{\alpha}_n = in\Omega\tilde{\alpha}_n - \omega_c\tilde{p}_n + 4g\omega_c\tilde{x}_n, \tag{C1a}$$

$$(\partial/\partial t)\tilde{p}_n = (\omega_c - i\kappa)\tilde{\alpha}_n + in\Omega\tilde{p}_n, \tag{C1b}$$

$$(\partial/\partial t)\tilde{x}_n = (in\Omega - \gamma_x)\tilde{x}_n - \omega_a\tilde{y}_n, \tag{C1c}$$

$$(\partial/\partial t)\tilde{y}_1 = \omega_a\tilde{x}_1 + (i\Omega - \gamma_y)\tilde{y}_1 - 8g^2\omega_c\left(\tilde{Z}_0\tilde{x}_1 + \tilde{z}_2^*\tilde{x}_3 + \tilde{x}_1^*\tilde{z}_2\right) + 2g\omega_c\left(\tilde{Z}_0\tilde{p}_1 + \tilde{z}_2^*\tilde{p}_3 + \tilde{p}_1^*\tilde{z}_2\right), \tag{C1d}$$

$$(\partial/\partial t)\tilde{y}_3 = \omega_a\tilde{x}_3 + (i3\Omega - \gamma_y)\tilde{y}_3 - 8g^2\omega_c\left(\tilde{Z}_0\tilde{x}_3 + \tilde{x}_1\tilde{z}_2\right) + 2g\omega_c\left(\tilde{Z}_0\tilde{p}_3 + \tilde{p}_1\tilde{z}_2\right), \tag{C1e}$$

$$(\partial/\partial t)\tilde{Z}_0 = -\gamma_z\left(\tilde{Z}_0 - Z_p\right) + 8g^2\omega_c\left(\tilde{x}_1^*\tilde{y}_1 + \tilde{x}_3^*\tilde{y}_3 + \text{c.c.}\right) - 2g\omega_c\left(\tilde{p}_1^*\tilde{y}_1 + \tilde{p}_3^*\tilde{y}_3 + \text{c.c.}\right), \tag{C1f}$$

$$(\partial/\partial t)\tilde{z}_2 = (i2\Omega - \gamma_z)\tilde{z}_2 + 8g^2\omega_c\left(\tilde{x}_1^*\tilde{y}_3 + \tilde{x}_1\tilde{y}_1 + \tilde{y}_1^*\tilde{x}_3\right) - 2g\omega_c\left(\tilde{p}_1^*\tilde{y}_3 + \tilde{p}_1\tilde{y}_1 + \tilde{y}_1^*\tilde{p}_3\right). \tag{C1g}$$

The equations to be solved are

$$0 = \left\{\frac{\Delta_{c,1}\Delta_{a,1}}{8g^2\omega_c\omega_a\Omega^2} + Z_p + \left[C_{|1|^21} + C_{|3|^21}|\eta|^2 + C_{(-1)^23}\eta\right]|\tilde{\alpha}_1|^2\right\}\tilde{\alpha}_1, \tag{C2a}$$

$$0 = \left\{\frac{\Delta_{c,3}\Delta_{a,3}}{8g^2\omega_c\omega_a\Omega^2} + 9Z_p + \left[C_{|1|^23} + C_{|3|^23}|\eta|^2 + C_{1^3}\eta^{-1}\right]|\tilde{\alpha}_1|^2\right\}\eta\tilde{\alpha}_1 e^{i2\theta}, \tag{C2b}$$

for unknown variables Ω, $|\tilde{\alpha}_1| \in \mathbb{R}$, and $\eta = e^{-i2\theta}\tilde{\alpha}_3/\tilde{\alpha}_1 \in \mathbb{C}$. The other quantities in Eqs. (C2) are defined as follows.

$$\Delta_{c,n} = \omega_c^2 - n^2\Omega^2 - i\kappa\omega_c, \tag{C3a}$$

$$\Delta_{a,n} = \omega_a^2 + (in\Omega - \gamma_x)(in\Omega - \gamma_y), \tag{C3b}$$

$$C_{|1|^2 1} = -\frac{\text{Re}[(\mathrm{i}\Omega - \gamma_x)\Delta_{c,1}]}{\gamma_z \omega_c \omega_a} + \frac{(\mathrm{i}\Omega - \gamma_x)\Delta_{c,1}}{2\omega_c \omega_a (\mathrm{i}2\Omega - \gamma_z)}, \tag{C4a}$$

$$C_{|3|^2 1} = -\frac{\text{Re}[(\mathrm{i}3\Omega - \gamma_x)\Delta_{c,3}]}{\gamma_z \omega_c \omega_a} + \frac{(\mathrm{i}3\Omega + \gamma_x)\Delta_{c,3}^* - 9(\mathrm{i}\Omega - \gamma_x)\Delta_{c,1}}{2\omega_c \omega_a (\mathrm{i}2\Omega + \gamma_z)}, \tag{C4b}$$

$$C_{(-1)^2 3} = -\frac{(\mathrm{i}3\Omega - \gamma_x)\Delta_{c,3} - 9(\mathrm{i}\Omega + \gamma_y)\Delta_{c,1}^*}{6\omega_c \omega_a (\mathrm{i}2\Omega - \gamma_z)} - \frac{3(\mathrm{i}\Omega + \gamma_x)\Delta_{c,1}^*}{2\omega_c \omega_a (\mathrm{i}2\Omega + \gamma_z)}, \tag{C4c}$$

$$C_{|1|^2 3} = -\frac{9\text{Re}[(\mathrm{i}\Omega - \gamma_x)\Delta_{c,1}]}{\gamma_z \omega_c \omega_a} + \frac{(\mathrm{i}3\Omega - \gamma_x)\Delta_{c,3} - 9(\mathrm{i}\Omega + \gamma_x)\Delta_{c,1}^*}{2\omega_c \omega_a (\mathrm{i}2\Omega - \gamma_z)}, \tag{C4d}$$

$$C_{|3|^2 3} = -\frac{9\text{Re}[(\mathrm{i}3\Omega - \gamma_x)\Delta_{c,3}]}{\gamma_z \omega_c \omega_a}, \tag{C4e}$$

$$C_{1^3} = -\frac{3(\mathrm{i}\Omega - \gamma_x)\Delta_{c,1}}{2\omega_c \omega_a (\mathrm{i}2\Omega - \gamma_z)}. \tag{C4f}$$

The other frequency components are obtained as

$$\tilde{\alpha}_3 = \eta \tilde{\alpha}_1 e^{\mathrm{i}2\theta}, \tag{C5a}$$

$$\tilde{p}_n = -\frac{\omega_c - \mathrm{i}\kappa}{\mathrm{i}n\Omega}\tilde{\alpha}_n, \tag{C5b}$$

$$\tilde{y}_n = -\frac{(\mathrm{i}n\Omega - \gamma_x)\Delta_{c,n}}{\mathrm{i}4ng\omega_c \omega_a \Omega}\tilde{\alpha}_n, \tag{C5c}$$

$$\tilde{x}_n = \frac{\omega_a}{\mathrm{i}n\Omega - \gamma_x}\tilde{y}_n, \tag{C5d}$$

$$\tilde{Z}_0 = Z_p + \frac{\mathrm{i}2g\Omega}{\gamma_z}\left(\tilde{\alpha}_1^* \tilde{y}_1 + 3\tilde{\alpha}_3^* \tilde{y}_3 - \text{c.c.}\right), \tag{C5e}$$

$$\tilde{z}_2 = -\frac{\mathrm{i}2g\Omega}{\mathrm{i}2\Omega - \gamma_z}\left(\tilde{\alpha}_1^* \tilde{y}_3 - \tilde{\alpha}_1 \tilde{y}_1 - 3\tilde{y}_1^* \tilde{\alpha}_3\right). \tag{C5f}$$

Appendix D: Other numerical results

The maps of "laser" solutions in the electric-dipole gauge are plotted in Fig. 4(a) for stronger electromagnetic interaction with matter $g' = 0.4$ and in Fig. 5(a) for lower cavity loss $\kappa = 0.001\omega_a$ compared with the parameters in the main text. Under these conditions, the bistability appears even in the electric-dipole gauge.

In Figs. 4-6, the dependence on the pure dephasing rate γ_{pure} is also shown. Figs. 4 and 5 are calculated in the electric-dipole gauge, and Figs. 6 is calculated in the Coulomb gauge (Fig. 6(a) is equivalent to Fig. 2(a) in the main text). The pure-dephasing ratio $\gamma_{\text{pure}}/\gamma_{\text{total}}$ is changed with keeping the total dissipation rates $\gamma_{\text{total}} = \gamma_\parallel + \gamma_{\text{pure}} = 0.15\omega_a$. In the conventional laser theory [6], the laser occurs under the following condition (determing the threshold Z_{th})

$$\frac{2g^2 \omega_a^2 Z_p}{\kappa\gamma_{\text{total}} - (\omega_c - \Omega)(\omega_a - \Omega)} > 1, \tag{D1}$$

where the oscillation frequency is obtained as

$$\Omega = \frac{\kappa\omega_a + \gamma_{\text{total}}\omega_c}{\kappa + \gamma_{\text{total}}}. \tag{D2}$$

In this way, the ω_c-range showing the conventional laser does not depends on the pure-dephasing ratio $\gamma_{\text{pure}}/\gamma_{\text{total}}$, and this tendency basically survives even in Figs. 4-6. Eq. (D1) is rewritten as

$$2g^2 \omega_a^2 Z_p > \kappa\gamma_{\text{total}}\left[1 + \left(\frac{\omega_a - \omega_c}{\gamma_{\text{total}} + \kappa}\right)^2\right]. \tag{D3}$$

This relation basically determines the ω_c-range of the "laser". Then, since we suppose $\kappa \ll \gamma_{\text{total}}$, the ω_c-range is enlarged by lowering κ and by heightening γ_{total} and g'.
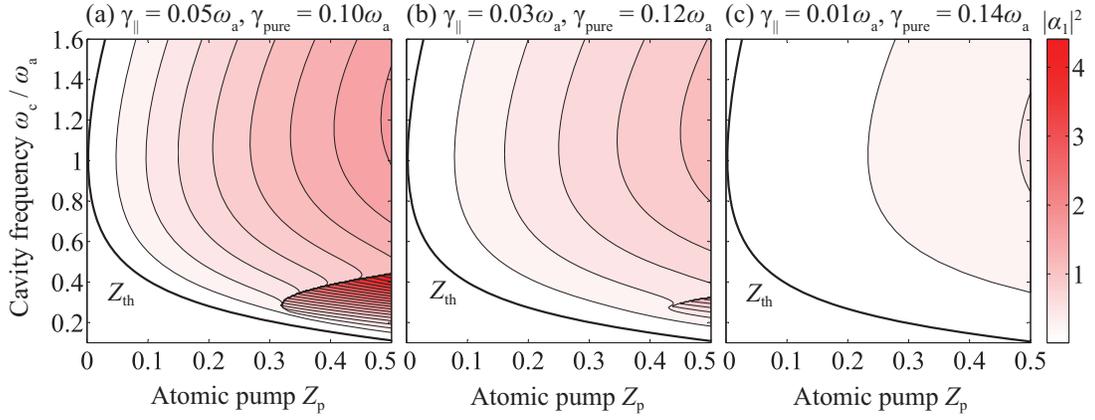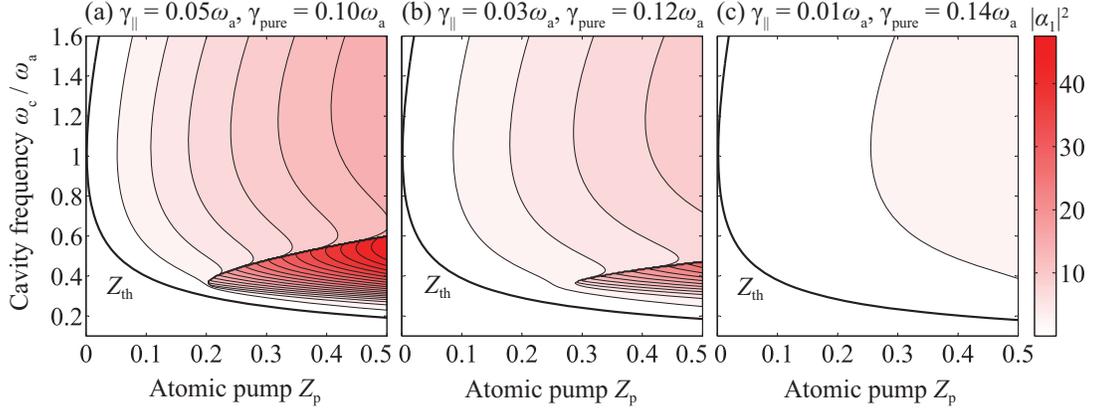
FIG. 4. Maps of "laser" solutions calculated in the electric-dipole gauge for $g' = 0.4$ and $\kappa = 0.01\omega_a$. The atomic dissipation rates are shown above the figures. The unconventional solutions appear for strong enough interaction and low enough cavity loss even in the electric-dipole gauge, while they disappear by increasing the ratio of the pure dephasing γ_{pure} with keeping the total dissipation rate $\gamma_{total} = \gamma_\parallel + \gamma_{pure}$.

FIG. 5. Maps of "laser" solutions calculated in the electric-dipole gauge for $g' = 0.15$ and $\kappa = 0.001\omega_a$. The atomic dissipation rates are shown above the figures. The unconventional solutions appear for strong enough interaction and low enough cavity loss even in the electric-dipole gauge, while they disappear by increasing the ratio of the pure dephasing γ_{pure} with keeping the total dissipation rate $\gamma_{total} = \gamma_\parallel + \gamma_{pure}$.
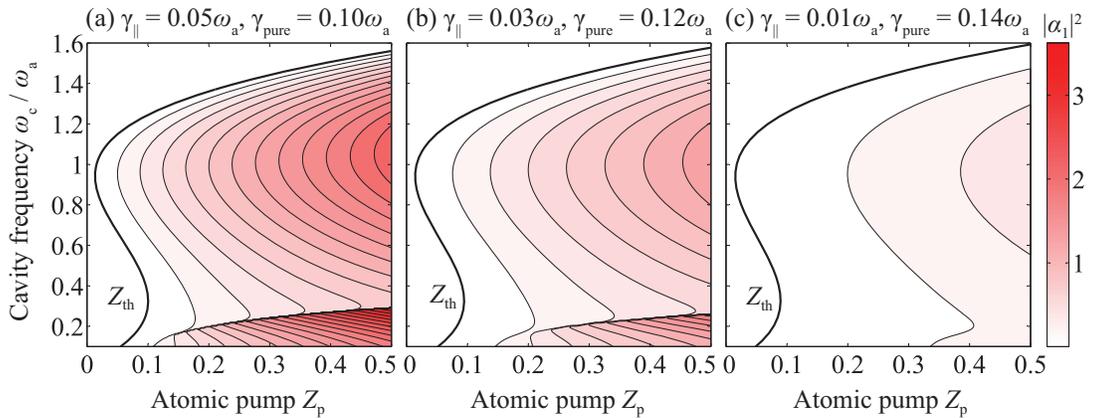

FIG. 6. Maps of "laser" solutions calculated in the Coulomb gauge for $g' = 0.15$ and $\kappa = 0.01\omega_a$. The atomic dissipation rates are shown above the figures (Panel (a) is equivalent to Fig. 2(a) in the main text). The unconventional solutions disappear by increasing the ratio of the pure dephasing γ_{pure} with keeping the total dissipation rate $\gamma_{total} = \gamma_\parallel + \gamma_{pure}$.
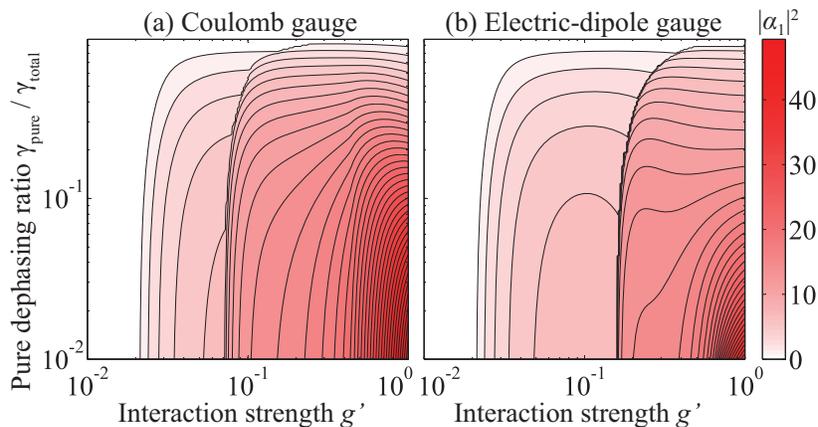
FIG. 7. Maps of "laser" solutions in (a) Coulomb gauge and (b) electric-dipole gauge. The color indicates the maximum $|\alpha_1|^2$ searched by changing ω_c. The larger value is chosen in the bistable case. The maximum $|\alpha_1|^2$ is plotted versus the interaction strength g' and the pure-dephasing ratio $\gamma_{\text{pure}}/\gamma_{\text{total}}$ with keeping $Z_p = 0.5$, $\gamma_{\text{total}} = 0.15\omega_a$, and $\kappa = 0.01\omega_a$.

In either calculation in Figs. 4-6, the bistable "laser" solutions are obtained for $\omega_c \sim \omega_a/3$, which is the requirement for the bistability as discussed in the main text. However, by increasing the pure-dephasing ratio $\gamma_{\text{pure}}/\gamma_{\text{total}}$, the unconventional solutions gradually disappear. This is because the amplitudes of the electromagnetic fields are diminished by increasing $\gamma_{\text{pure}}/\gamma_{\text{total}}$ as clearly seen in the figures. Especially, the third harmonic amplitudes are diminished more drastically (not shown in the figures), because they appear as similar as the nonlinear optical effect. For much lower $\gamma_{\text{pure}}/\gamma_{\text{total}}$, the bistability appears more clearly (not shown in the figures). Then, for obtaining the bistability, we should prepare low enough κ and γ_{pure} and high enough $\gamma_{\parallel}$ and g'.

In Figs. 7, we plot the maximum $|\alpha_1|^2$ searched by changing ω_c in the two gauges. The larger value is chosen in the bistable case, and it is plotted versus the interaction strength g' and the pure dephasing ratio $\gamma_{\text{pure}}/\gamma_{\text{total}}$ with keeping $Z_p = 0.5$, $\gamma_{\text{total}} = 0.15\omega_a$, and $\kappa = 0.01\omega_a$. The relatively large $|\alpha_1|^2$ for strong enough g' indicates the existence of the bistability. In either gauge, whereas the bistability is obtained clearly for low enough $\gamma_{\text{pure}}/\gamma_{\text{total}}$, the visibility is lowered with the increase in $\gamma_{\text{pure}}/\gamma_{\text{total}}$. This tendency indicates the disappearance of the bistability demonstrated in Figs. 4-6. Whereas the bistability is obtained even for the relatively high $\gamma_{\text{pure}}/\gamma_{\text{total}} \sim 0.8$ as shown in Figs. 4-6, stronger g' is required for the bistability as seen in Figs. 7. The bistable region is not largely enhanced even in the limit of $\gamma_{\text{pure}}/\gamma_{\text{total}} \to 0$. This is because the pure dephasing ratio $\gamma_{\text{pure}}/\gamma_{\text{total}}$ basically does not change the parameter region showing $\Omega \sim \omega_a/3$, that is determined by Eq. (D3).

[1] T. H. Maiman, Nature **187**, 493 (1960).
[2] A. Schawlow and C. Townes, Phys. Rev. **112**, 1940 (1958).
[3] H. Haken, *Light and Matter Ic: Laser Theory*, Vol. XXV/2c of *Encyclopedia of Physics / Optics* (Springer-Verlag, Berlin, Heidelberg, New York, 1970).
[4] H. Haken, *Laser Light Dynamics*, Vol. 2 of *Light* (North Holland, Amsterdam, 1985).
[5] M. O. Scully and M. S. Zubairy, *Quantum Optics*, (Cambridge University Press, Cambridge, 1997).
[6] C. W. Gardiner and P. Zoller, *Quantum Noise* (Springer-Verlag, Berlin, 2004), Third edition.
[7] C. Ciuti, G. Bastard, and I. Carusotto, Phys. Rev. B **72**, 115303 (2005).
[8] G. Gunter, A. A. Anappara, J. Hees, A. Sell, G. Biasiol, L. Sorba, S. De Liberato, C. Ciuti, A. Tredicucci, A. Leitenstorfer, and R. Huber, Nature **458**, 178 (2009).
[9] A. A. Anappara, S. De Liberato, A. Tredicucci,

C. Ciuti, G. Biasiol, L. Sorba, and F. Beltram, Phys. Rev. B **79**, 201303 (2009).
[10] Y. Todorov, A. M. Andrews, I. Sagnes, R. Colombelli, P. Klang, G. Strasser, and C. Sirtori, Phys. Rev. Lett. **102**, 186402 (2009).
[11] Y. Todorov, A. M. Andrews, R. Colombelli, S. De Liberato, C. Ciuti, P. Klang, G. Strasser, and C. Sirtori, Phys. Rev. Lett. **105**, 196402 (2010).
[12] T. Niemczyk, F. Deppe, H. Huebl, E. P. Menzel, F. Hocke, M. J. Schwarz, J. J. Garcia-Ripoll, D. Zueco, T. Hummer, E. Solano, A. Marx, and R. Gross, Nat. Phys. **6**, 772 (2010).
[13] A. Fedorov, A. K. Feofanov, P. Macha, P. Forn-Díaz, C. J. P. M. Harmans, and J. E. Mooij, Phys. Rev. Lett. **105**, 060503 (2010).
[14] P. Forn-Díaz, J. Lisenfeld, D. Marcos, J. J. García-Ripoll, E. Solano, C. J. P. M. Harmans, and J. E. Mooij, Phys. Rev. Lett. **105**, 237001 (2010).

[15] T. Schwartz, J. A. Hutchison, C. Genet, and T. W. Ebbesen, Phys. Rev. Lett. **106**, 196405 (2011).

[16] M. Porer, J.-M. Ménard, A. Leitenstorfer, R. Huber, R. Degl'Innocenti, S. Zanotto, G. Biasiol, L. Sorba, and A. Tredicucci, Phys. Rev. B **85**, 081302 (2012).

[17] G. Scalari, C. Maissen, D. Turčinková, D. Hagenmüller, S. De Liberato, C. Ciuti, C. Reichl, D. Schuh, W. Wegscheider, M. Beck, and J. Faist, Science **335**, 1323 (2012).

[18] Y. Todorov and C. Sirtori, Phys. Rev. B **85**, 045304 (2012).

[19] Y. Todorov, Phys. Rev. B **89**, 075115 (2014).

[20] C. Cohen-Tannoudji, J. Dupont-Roc, and G. Grynberg, *Photons and Atoms: Introduction to Quantum Electrodynamics* (Wiley, New York, 1989).

[21] J. Keeling, J. Phys.: Condens. Matter **19**, 295213 (2007).

[22] A. Vukics, T. Grießer, and P. Domokos, Phys. Rev. Lett. **112**, 073601 (2014).

[23] M. Bamba and T. Ogawa, Phy. Rev. A **90**, 063825 (2014).

[24] The last terms in Eqs. (1) and (2) are called the A^2 and P^2 terms, respectively; $(\hat{a}+\hat{a}^\dagger)$ and $\hat{\sigma}_\lambda^x$ correspond to the vector potential $\hat{A}(\boldsymbol{r})$ and the transverse atomic polarization $\hat{P}_\perp(\boldsymbol{r})$, respectively. In the presence of these terms, we do not have the superradiant phase transition in equilibrium situations even in the ultrastrong regime [23, 26–30], while the laser can be realized in non-equilibrium situations regardless of whether the interaction is ultrastrong.

[25] Due to the two-level and single-mode approximations, the Hamiltonians (1) and (2) are not equivalent with each other through the transformation with unitary operator $\hat{U} = \exp[-\mathrm{i}g(\hat{a} + \hat{a}^\dagger)\sum_\lambda \hat{\sigma}_\lambda^x/\sqrt{N}]$, whereas the original Hamiltonian can be transformed to each other under the long-wavelength approximation [20–23]. Since $\hat{\sigma}_\lambda^x$ and $(\hat{a}+\hat{a}^\dagger)$ are commutable with $\hat{U}$, the system-environment couplings mediated by them give the same contribution in both gauges. However, $\hat{\sigma}_\lambda^z$ mediating the pure dephasing is not commutable with $\hat{U}$.

[26] K. Rzążewski, K. Wódkiewicz, and W. Żakowicz, Phys. Rev. Lett. **35**, 432 (1975).

[27] K. Rzążewski and K. Wódkiewicz, Phys. Rev. A **13**, 1967 (1976).

[28] M. Yamanoi, Phys. Lett. A **58**, 437 (1976).

[29] V. Emeljanov and Y. Klimontovich, Phys. Lett. A **59**, 366 (1976).

[30] M. Yamanoi and M. Takatsuji, *Coherence and quantum optics IV: proceedings of the fourth Rochester Conference on Coherence and Quantum Optics*, edited by L. Mandel and E. Wolf (Plenum Press, New York, 1978), pp. 839–850.

[31] M. Bamba and T. Ogawa, Phys. Rev. A **89**, 023817 (2014).

[32] See the supplemental material.

[33] Since the couplings with heat baths are mediated by $\{\hat{\sigma}_\lambda^x\}$, X does not feel the influence of them ($\gamma_x = \gamma_{\mathrm{pure}}$), while Y decays with rate $\gamma_y = \gamma_\parallel + \gamma_{\mathrm{pure}}$. In this treatment, we partially used the pre-trace RWA [31] for simplicity (see also the supplemental material [32]). $X = Y = 0$ and $Z = Z_\mathrm{p}$ are guaranteed below the threshold even in this treatment. In the same manner, the loss terms appear only in equations of motion of Π. If the pre-trace RWA is fully applied, the results in this paper are changed quantitatively but slightly.

[34] A. Ridolfo, M. Leib, S. Savasta, and M. J. Hartmann, Phys. Rev. Lett. **109**, 193602 (2012).

[35] M. Koschorreck, R. Gehlhaar, V. G. Lyssenko, M. Swoboda, M. Hoffmann, and K. Leo, Appl. Phys. Lett. **87**, 181108 (2005).

[36] Z. Han, H.-S. Nguyen, F. Réveret, K. Abdel-Baki, J.-S. Lauret, J. Bloch, S. Bouchoule, and E. Deleporte, Appl. Phys. Express **6**, 106701 (2013).

[37] G. M. Akselrod, E. R. Young, K. W. Stone, A. Palatnik, V. Bulović, and Y. R. Tischler, Phys. Rev. B **90**, 035209 (2014).

[38] In contrast to the multi-mode lasers [4], the relative phases between the multiple harmonics are fixed for the "laser" in the ultrastrong regime, while an absolute phase can be chosen arbitrarily in the present calculation.

[39] The stability of the oscillating steady states are checked against small deviations of $|\alpha_1|$, Z_0 and $\mathrm{e}^{-\mathrm{i}2\theta}z_2$, where $\mathrm{e}^{\mathrm{i}\theta} = \alpha_1/|\alpha_1|$. The equations of motion are reduced to the ones of these variables, and the phase θ of α_1 is also eliminated, because it is not determined by our equations of motion.

[40] Even if the interaction survives in the "laser", it is different from the polariton lasers [41], i.e., the emission from polariton condensates.

[41] A. Imamoğlu, R. J. Ram, S. Pau, and Y. Yamamoto, Phys. Rev. A **53**, 4250 (1996).

[42] F. Bassani, J. J. Forney, and A. Quattropani, Phys. Rev. Lett. **39**, 1070 (1977).

[43] For making the population inversion, we use the atomic levels that interact with the two levels of interest through non-radiative transitions. These levels can be close to the two levels of interest energetically.

[44] The multi-stability in the conventional multi-mode laser shows drastic changes of the emission spectra, while peak positions are not strongly changed in the bistability originating from the lack of the RWA as seen in Fig. 2(f).

[45] Non-classical states of light are generated usually by applying nonlinear optical processes (with showing, e.g., a bistability) to a coherent state [5, 6]. For direct lasing of the non-classical states, we basically need special tricks, such as noise-suppressed pumping [46, 47].

[46] Y. Yamamoto, S. Machida, and O. Nilsson, Phys. Rev. A **34**, 4025 (1986).

[47] S. Machida, Y. Yamamoto, and Y. Itaya, Phys. Rev. Lett. **58**, 1000 (1987).

[48] D. J. Jones, S. A. Diddams, J. K. Ranka, A. Stentz, R. S. Windeler, J. L. Hall, and S. T. Cundiff, Science **288**, 635 (2000).

[49] O. Astafiev, K. Inomata, A. O. Niskanen, T. Yamamoto, Y. A. Pashkin, Y. Nakamura, and J. S. Tsai, Nature **449**, 588 (2007).